Adaptive Self-Preservation in Flocking Systems: How Dynamic Risk Thresholds Shape Collective Safety

Jiaman Li[0009−0009−9322−0400] and William G. Kennedy[0000−0001−9238−1215]

George Mason University, Fairfax VA 22030, USA
jli30@gmu.edu, wkennedy@gmu.edu

Abstract. Can simple local experiences, such as a near-collision, shape how risk is distributed within a group, even when agents have no memory, communication, or global coordination? Traditional flocking models assume fixed behavioral parameters, yet real organisms often become more cautious after close encounters and relax only gradually when conditions feel safe. We formalize a memoryless threshold adaptation rule where agents increase their collision threshold by α following a near-miss but decay it by β during safety, with the α/β ratio acting as a control parameter. Through systematic experiments on NetLogo's flocking model ($N = 540$ runs), we identify three distinct behavioral regimes determined by α/β: homogeneous risk-aversion ($\alpha/\beta \geq 10$), stable differentiated equilibrium ($\alpha/\beta \approx 5$), and collapse to risk-neutrality ($\alpha/\beta \leq 2.5$). In particular, effective self-organization arises primarily within a narrow parameter window, where identical agents develop heterogeneous risk tolerances through interaction alone. This reveals a fragility in adaptive decentralized systems: simple local rules can generate emergent safety structures, with maximum heterogeneity (SD = 0.71) at regime boundaries, but stable differentiation occurs only within tightly bounded parameter regimes, challenging the assumption that minimal mechanisms guarantee robustness.

Keywords: Adaptive self-preservation · Flocking · Emergent heterogeneity · Phase transitions · Agent-based modeling

1 Introduction

In many complex systems, collective behavior emerges without any centralized leader. Examples range from bird flocks and fish schools to robot swarms and autonomous vehicle platoons. Each individual follows simple local interaction rules, yet the collective exhibits organized motion and coherent patterns [22]. This reflects a core principle of complexity science: macro-order arising from micro-interactions [18].

The classic Boids model introduced by Reynolds [17] first demonstrated how three simple rules, concerning alignment, cohesion, and separation, can produce lifelike flocking behavior in computer simulations. In this model, each agent (the

boids) aligns its direction with nearby neighbors (alignment), steers toward the local center of its group (cohesion), and turns away if others come too close (separation). No agent is designated as a leader; instead, the flock structure emerges spontaneously as each agent follows the same rules. Uri Wilensky's NetLogo Flocking model [24, 25] further popularized this framework, providing an accessible platform to experiment with how adjusting rule parameters affects group dynamics.

Traditional flocking models assume that all agents use identical, fixed behavioral parameters throughout the simulation. However, real individuals (animals or people) adapt their behavior based on experience. An animal that survives a near-collision with a predator becomes more sensitive [9]; a pedestrian who nearly bumps into someone adjusts their personal space [15]. Learning and adaptation are fundamental to biological self-preservation [13].

Recent work has examined parameter sensitivity in flocking systems [6] and adaptive responses to environmental changes [16], but most standard boid agents lack cognitive flexibility to regulate risk . This raises an important question: How do individual adaptive responses affect collective dynamics? When agents can modify their own safety thresholds based on experience, do new patterns emerge? Does the population develop heterogeneous risk tolerances, even when starting from identical conditions?

This paper asks a basic question: Can agents learn to be cautious or relaxed through simple feedback from their environment, without any memory of past events or communication with neighbors? We model this using a threshold that goes up when an agent has a near-miss, and slowly decays when things feel safe. The key is the ratio α/β : how fast agents react to danger versus how fast they forget about it.

We identify the α/β ratio as a control parameter governing phase transitions in adaptive flocking. Through systematic experiments (N=540 runs), we demonstrate three distinct regimes: homogeneous risk-aversion ($\alpha/\beta \geq 10$), stable differentiated equilibrium ($\alpha/\beta \approx 5$), and collapse to risk-neutrality ($\alpha/\beta \leq 2.5$). Stable differentiation emerges only within a narrow parameter window, with maximum heterogeneity (SD = 0.71) at regime boundaries. This reveals fragility: small changes in the adaptation-decay balance trigger abrupt phase transitions.

2 Related Work

2.1 Classical Flocking and Collective Motion Models

Reynolds' Boids model [17] established the foundation for computational flocking, demonstrating that three local rules (alignment, cohesion, separation) are sufficient to produce realistic collective patterns. Vicsek et al. [23] introduced a minimal model showing phase transitions between ordered and disordered collective motion. Couzin et al. [4, 3] extended this work by defining interaction zones and studying how leadership emerges in complex moving groups. Wilensky's NetLogo implementation [24, 25] further popularized these models, making them accessible for interdisciplinary research.

Recent work shows that flocking birds use topological interactions[1] and that individual differences affect collective patterns [14], challenging classical homogeneity assumptions and motivating adaptive parameter models such as the one studied here.

2.2 Parameter Sensitivity and Adaptive Dynamics

Extensive research examines how parameter variations affect flocking stability and emergence. Farkas and Wang [6] conducted systematic sensitivity analysis of flocking parameters including speed, distance thresholds, noise, and delays, showing that small parameter changes can induce qualitative transitions in collective behavior. This establishes a framework for understanding how threshold variations influence system-level dynamics.

Also, adaptation is observed in nature: predation threats change individual sensitivity [16], and individual differences in decision-making create behavioral heterogeneity even among genetically identical organisms [10, 21]. Our work models how such adaptive sensitivity emerges through simple, memoryless feedback rules, examining the micro-macro link between individual adaptation and collective heterogeneity.

2.3 Optimization-Based Collision Avoidance

Collision avoidance in multi-agent systems has been addressed through optimization and learning methods. Recent advances in Multi-Agent Reinforcement Learning (MARL) enable agents to discover complex coordination strategies [11, 19]. These methods can optimize global objectives, but require extensive training, reward engineering, and computational resources.

Our approach serves a different purpose: to understand the minimal mechanism by which local adaptive rules generate emergent heterogeneity. By using memoryless feedback (Equation 1, described in Section 3), we isolate the effects of asymmetric adaptation without optimization overhead. This makes our model suitable for both mechanistic inquiry into adaptive collective dynamics.

2.4 Self-Preservation and Cognitive Heuristics

In contrast to heavy optimization, research on biological systems suggests that organisms often rely on fast, simple cognitive heuristics [8]. Moussaïd et al. [15] showed that pedestrians follow rules like "stop if another step would lead to a collision" rather than computing optimal paths. Seitz et al. [20] demonstrated how such heuristics explain spatial movement patterns.

Our approach differs from previous work in focus rather than capability. While optimization methods prioritize task performance and fixed-parameter models assume stability, we investigate how local adaptive rules generate emergent heterogeneity, which is a question central to understanding collective behavior in biological and artificial systems.

3 Model

3.1 Base Model: NetLogo Flocking

We built our simulation using NetLogo, a platform well-suited for agent-based modeling of complex systems. Our starting point is the NetLogo library's Flocking model, which implements Reynolds' boid rules [24]. This model operates on a 2D toroidal grid with N agents (wrapping around edges) and advances in discrete time steps ("ticks"). Each agent (bird) updates its heading each tick based on local perceptions within a certain radius. By default, the flocking model includes three core behaviors:

- **Alignment:** a bird tends to turn so that it is moving in the same direction as nearby birds (to align direction with the group).
- **Cohesion:** move toward the average position of nearby birds (to stay with the group).
- **Separation:** a bird will turn to avoid another bird that gets too close (to avoid crowding or collisions).

The separation rule takes priority: when triggered, it overrides alignment and cohesion. Each rule has a maximum turn rate limiting how sharply agents can adjust their heading per time step.

3.2 Adaptive Self-Preservation Mechanism

We extend the base flocking model by giving each agent i a dynamic personal collision threshold $T_i(t) \in [T_{\min}, T_{\max}]$. This threshold determines the agent's risk sensitivity: a near-miss is detected when the distance to the nearest neighbor falls below $T_i(t)$.

Memoryless Feedback Control: To regulate this threshold, we adopt a linear adjustment rule based on two design principles. First, the update should be memoryless, which means that only the current state matters, not the accumulation of past experiences. This reflects biological constraints: organisms often react to immediate stimulation rather than keeping detailed records of the past [8]. Second, the rule should implement asymmetric learning, rapid increase upon threat detection but gradual decay during safety, consistent with a risk-averse strategy [13]. The update rule is formalized as:

$$T_i(t+1) = T_i(t) + \alpha \cdot I_{\text{near-miss}} - \beta \cdot (1 - I_{\text{near-miss}}) \tag{1}$$

subject to $T_{\min} \leq T_i(t+1) \leq T_{\max}$, where:

- State**:** Only current threshold $T_i(t)$ persists (memoryless property)
- Stimulus**:** Binary near-miss detection $I_{\text{near-miss}} \in \{0, 1\}$
- Response**:** Increase by α if danger, decrease by β if safe

Boundary Constraints: The threshold bounds are calibrated to biological and physical constraints imposed by the base flocking model. We set the lower bound $T_{\min} = 0.5$ (10% of vision, 50% of minimum-separation) represents extreme risk tolerance, ensuring agents maintain basic collision avoidance. The upper bound is set to $T_{\max} = 2.0$ (40% of vision, 200% of minimum-separation) based on Weber's Law[7], preventing agents from reacting to ecologically irrelevant distant neighbors. The resulting 4-fold range ($T_{\max}/T_{\min} = 4.0$) mirrors observed behavioral variability in animal groups [5].

Adaptation Rate (α) and Decay Rate (β): We set $\alpha = 0.05$ (baseline) based on animal learning studies. Griffin et al. [9] found birds develop lasting predator vigilance after 5–10 dangerous encounters. With $\alpha = 0.05$, agents require approximately 20 near-misses to meet the full threshold range from $T_{\min}$ to $T_{\max}$ (since $\Delta T = T_{\max} - T_{\min} = 1.5$, requiring $1.5/0.05 = 30$ increments, or $\sim$20 near-misses accounting for boundary effects).

We set $\beta = 0.01$ (baseline), yielding $\alpha/\beta = 5$. This specific ratio is grounded in Loss Aversion and Prospect Theory. Kahneman & Tversky's [12] Prospect Theory demonstrates that organisms weight losses approximately 2–3$\times$ more heavily than equivalent gains. In our context, a "loss" represents a near-miss, while a "gain" represents safety. The evolutionary theory suggests that strategies favoring false positives (over caution) over false negatives (missing a threat) typically use ratios ≥ 2. Our choice of $\alpha/\beta = 5$ is conservative but consistent with a risk-averse strategy[13].

Technically, this asymmetry ($\alpha \gg \beta$) implements the "once bitten, twice shy" behavioral principle. With $\alpha = 0.05$ and $\beta = 0.01$, a single near-miss increases the threshold by 5%, but requires 5 consecutive safe time steps to decay by the same amount. This creates a threshold with ratchet effect: it is easy to become cautious but hard to relax, which is exactly the pattern observed in animal risk assessment under predation pressure [2].

3.3 Visual Feedback and Key Metrics

To visualize emergent heterogeneity, we use a dynamic coloring system. Agents in a near-miss state turn red, providing immediate feedback on system risk. In adaptive mode, safe agents' colors indicate their threshold level: darker colors represent higher thresholds (more cautious), lighter colors represent lower thresholds (more risk-tolerant).

We measure four outcomes:

- Near-miss rate: Percentage of agents currently in near-miss state.
- Mean threshold: Average T_i across the population.
- Threshold SD: Standard deviation of T_i , which is a proxy for behavioral heterogeneity.
- Cohesion index: Average number of neighbors per agent with vision radius.

4 Experimental Design

We conducted three experiments to address our research questions, totaling 540 simulation runs with 30 replications per condition and 500 time steps each.

4.1 Experiment 1: Fixed vs Adaptive Comparison

We compared fixed threshold mode (agents use constant T) with adaptive mode (agents update T_i via Equation 1) to evaluate whether the adaptive mechanism offers advantages over fixed parameter settings. We utilized a 2×3 factorial design crossing mode (Fixed vs. Adaptive) with initial threshold $T_{\text{init}} \in \{0.75, 1.0, 1.5\}$. These initial values represent risk-tolerant, neutral, and risk-averse baselines relative to the model's default minimum separation (1.0). The primary objective is to test for convergence: specifically, whether adaptive agents self-organize to a common safety equilibrium regardless of their starting conditions, which is a key standard for robust decentralized systems.We hypothesized that the adaptive mode produces emergent heterogeneity (threshold SD > 0), unlike fixed mode.

4.2 Experiment 2: Parameter Sensitivity

To understand the impact of learning dynamics, we varied the adaptation rate $\alpha \in \{0.02, 0.05, 0.10\}$ and the decay rate $\beta \in \{0.005, 0.01, 0.02\}$ in a full factorial design. This explores three different asymmetry ratios: $\alpha/\beta \approx 1$ –2 (near-symmetric that test necessity of asymmetry), $\alpha/\beta \approx 5$ (moderate asymmetry which is the baseline and match loss-aversion literature), and $\alpha/\beta \approx$ 10–20 (strong asymmetry, extreme conservatism). This design allows us to isolate the interaction effects between learning and decay rates on system stability.

4.3 Experiment 3: Density Robustness

To assess scalability, we tested the population levels of $N \in \{100, 200, 400\}$, while keeping the adaptation parameters constant ($\alpha = 0.05$, $\beta = 0.01$). These levels are related to different ecological conditions: sparse (4 agents/100 patches, flocks loosely coupled, collisions rare), medium (8 agents/100 patches, natural flock density [1]), and dense (16 agents/100 patches), crowded conditions [15]). This 4-fold variation tests whether the adaptive mechanism remains robust as the system transitions from isolated movement to continuous interaction.

4.4 Control Parameters and Analysis Methods

All other parameters were held constant: vision = 5 patches, minimum separation = 1 patch, max-align-turn rate = 5°/step, max-cohere-turn rate = 3/step, max-separate-turn rate = 1.5°/step, $T_{\min} = 0.5$, $T_{\max} = 2.0$.

We computed descriptive statistics (mean, SD) by condition. Statistical tests included independent samples t-tests (Exp 1), two-way ANOVA with interaction (Exp 2), and one-way ANOVA with Tukey HSD post-hoc tests (Exp 3). Effect sizes (Cohen's d, partial η^2) assessed practical significance.

5 Results

5.1 Experiment 1: Adaptive Agents Develop Heterogeneity

We first examined whether identical agents could develop differentiated behaviors solely through interaction. Table 1 summarizes the comparison between fixed-parameter baselines and the adaptive mode,

Table 1. Experiment 1 Results: Fixed vs Adaptive Comparison

Mode	Init T	Near-Miss (%)	Mean T	SD T	n
Fixed	0.75	23.4 ± 3.0	0.75	0.000	30
Fixed	1.00	40.0 ± 4.5	1.00	0.000	30
Fixed	1.50	87.5 ± 2.0	1.50	0.000	30
Adaptive	0.75	94.5 ± 1.2	1.95	0.251	30
Adaptive	1.00	93.9 ± 1.5	1.94	0.268	30
Adaptive	1.50	94.1 ± 1.7	1.94	0.259	30

In fixed mode, the standard deviation (SD) of thresholds was zero by definition. In adaptive mode, threshold SD ranged from 0.251 to 0.268 across initial conditions, indicating significant heterogeneity. A one-sample t-test confirmed that adaptive threshold SD was significantly greater than zero: $t(89) = 57.44$, $p = 3.92 \times 10^{-72}$ (Figure 1). This demonstrates that identical agents following identical rules develop differentiated risk tolerances purely through experiential feedback.

Independent samples t-tests comparing fixed vs adaptive modes at each initial threshold level revealed extremely large effect sizes: $T_{\text{init}} = 0.75$: $t = 119.11$, $p = 5.04 \times 10^{-71}$, Cohen's $d = 30.75$; $T_{\text{init}} = 1.0$: $t = 62.46$, $p = 6.78 \times 10^{-55}$, $d = 16.13$; $T_{\text{init}} = 1.5$: $t = 13.80$, $p = 5.73 \times 10^{-20}$, $d = 3.56$. These effect sizes confirm that the adaptive mechanism fundamentally transforms system behavior. Regardless of the initial threshold (0.75, 1.0, or 1.5), the adaptive agents

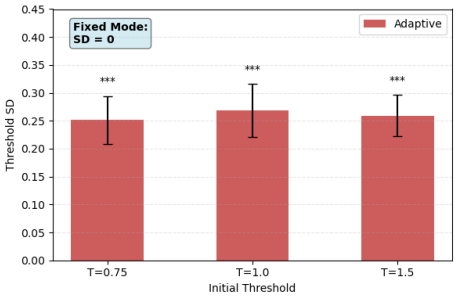

Fig. 1. Exp 1 Emergent Heterogeneity

converged to nearly identical mean thresholds of 1.94–1.95, close to $T_{\max} = 2.0$.

This shows that even agents initialized with risk-tolerant thresholds ($T_{\text{init}} = 0.75$, well below minimum-separation) rapidly adapted to safe levels. The convergence is remarkably tight (SD < 0.01 across initial conditions), indicating a robust equilibrium.

Interestingly, the adaptive mode exhibited significantly higher near-miss rates (93.9–94.5%) compared to fixed modes (23.4–87.5%), reflecting increased situational awareness rather than danger: near-misses trigger at larger safety margins (≈ 1.95 patches), preventing actual collisions.

5.2 Experiment 2: What the α/β Ratio Really Does

To map out when the system works and when it breaks, we conducted a full factorial sweep of the adaptation rate (α) and decay rate (β). Tables 2 and 3 present mean thresholds and heterogeneity across parameter combinations, visualized in Figures 2. The Two-way ANOVA revealed significant main effects

Table 2. Mean Threshold

	Decay Rate (β)		
α	0.005	0.010	0.020
0.02	1.74	0.68	0.51
0.05	1.99	1.95	1.25
0.10	1.99	1.99	1.96

Table 3. Threshold SD

	Decay Rate (β)		
α	0.005	0.010	0.020
0.02	0.55	0.47	0.05
0.05	0.09	0.25	**0.71**
0.10	0.08	0.11	0.22

of α ($F(2, 261) = 22193.79$, $p < .001$, $\eta_p^2 = 0.994$) and β ($F(2, 261) = 9257.94$, $p < .001$, $\eta_p^2 = 0.986$), and a significant interaction ($F(4, 261) = 3864.55$, $p < .001$, $\eta_p^2 = 0.983$). The magnitude of these effects suggests that the ratio α/β dictates the system's phase. We identify three distinct behavioral regimes:

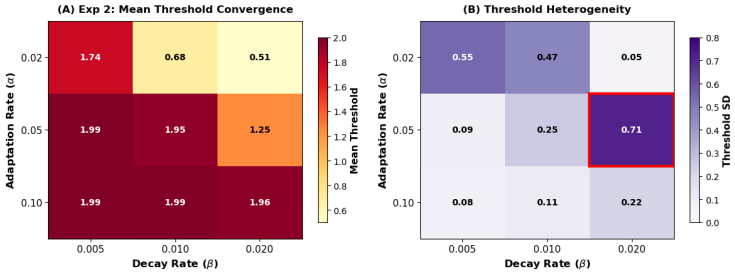

Fig. 2. Exp 2: Parameter Sensitivity Analysis

Regime: Homogeneous Risk-Aversion ($\alpha/\beta \geq 10$). When $\alpha/\beta \geq 10$ thresholds converge rapidly to $T_{\max} = 2.0$ (mean = 1.99, SD = 0.08–0.09). All agents become cautious, producing homogeneous risk-averse populations.

Regime: Stable Differentiated Equilibrium ($\alpha/\beta \approx 5$). When $\alpha/\beta = 5$ ($\alpha = 0.05$, $\beta = 0.01$), the baseline condition, thresholds converge to high values (mean = 1.95, SD = 0.25), balancing collective safety with individual variation.

Regime: Collapse to Risk-Neutrality ($\alpha/\beta \leq 2.5$). When $\alpha/\beta \leq 2.5$, thresholds decay to $T_{\min}$ (mean = 0.51–0.68), collapsing to risk-neutrality as decay overpowers adaptation. At high decay rates ($\beta = 0.02$), heterogeneity patterns show non-monotonic behavior (Table 4, third column), suggesting complex interactions that require further investigation.

Figure 2B reveals a pattern that maximum heterogeneity (SD = 0.71) at $\alpha/\beta = 2.5$, precisely at the phase boundary between stable differentiated equilibrium and collapse. At this point, early near-miss experiences increase into lasting behavioral differences, producing maximal differentiation. The key finding from this experiment is that the α/β ratio, not absolute parameter values, determines the emergent behavior.

5.3 Experiment 3: Robust Across Densities

Finally, we evaluated the system's performance across varying population densities ($N \in \{100, 200, 400\}$). Results are summarized in Table 4, visualized as figure 3.

Table 4. Experiment 3: Density Robustness Results

Population	Near-Miss (%)	Mean T	SD T
100	81.5 ± 6.1	1.74	0.53
200	90.9 ± 1.7	1.89	0.37
400	95.5 ± 1.1	1.97	0.19

One-way ANOVA showed a significant effect of population density on near-miss rates: $F(2, 87) = 111.0$, $p = 1.13 \times 10^{-24}$, $\eta^2 = 0.718$ (large effect). Post-hoc Tukey HSD tests confirmed that all pairwise comparisons were significant ($p < .001$): 100 vs 200 (mean difference = 9.38%), 100 vs 400 (14.05%), 200 vs 400 (4.67%). Although the adaptive mechanism functioned robustly throughout the 4-fold density range, the specific outcomes exhibited density dependence. Furthermore, the system shows the adaptive constraint. As shown in Fig.3, when density increases from 100 to 400 agents, the mean threshold automatically rises ($1.74 \rightarrow 1.97$), while heterogeneity declines ($SD : 0.53 \rightarrow 0.19$).

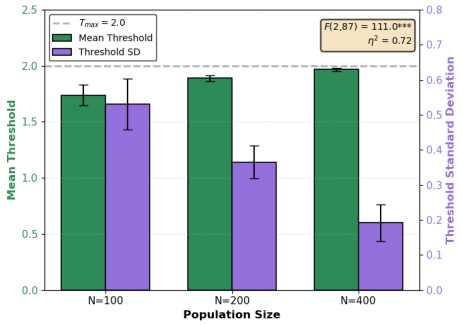

Fig. 3. Exp 3: Density Robustness

This indicates a functional trade-off: sparse environments ($N = 100$) allow diverse, relaxed thresholds, while dense environments ($N = 400$) force uniform high-safety standards. The adaptive mechanism enables automatic scalability.

6 Discussion

All agents begin with identical rules and parameters, yet develop heterogeneous risk tolerances through experience. This shows how individual variation can arise without predisposition, which is a key principle in complexity science. Differentiation emerges from the interaction between identical agents and their stochastic environments. Our findings align with recent observations that behavioral heterogeneity can emerge even among genetically identical individuals [10] and that individual differences shape collective outcomes [14, 21]. However, previous work typically assumes pre-existing heterogeneity, whereas our model demonstrates how it can emerge dynamically from experience.

The key to this emergent stability is the asymmetry between the adaptation and decay rates ($\alpha \gg \beta$). This models the biological observation that negative experiences (near-misses) have lasting impact, while positive experiences (safety) are quickly forgotten. The "once bitten, twice shy" principle appears to be a fundamental mechanism underlying self-preservation. The key role of the α/β ratio aligns with the findings of Farkas & Wang [6] that flocking systems exhibit nonlinear sensitivity to parameter combinations. Their work on fixed parameters complements our analysis of adaptive thresholds, together showing a comprehensive study of how sensitivity, whether static or dynamic, determines collective behavior.

From a practical perspective, our heuristic approach requires no training and enables immediate online adaptation, making it suitable for resource-constrained systems. While learning methods can optimize complex objectives, simple rules may suffice when the goal is mechanistic understanding.

The results are specific to 2D environments with binary detection and no communication, which are deliberate simplifications to isolate asymmetric feedback effects. Extensions to 3D, continuous perception, or communication represent future directions. Our contribution is to demonstrate the minimal mechanism

for emergent heterogeneity and to reveal its fragility within a narrow parameter window.

7 Conclusion

This study addressed the internal limitation of traditional flocking models: the reliance on static behavioral parameters that do not adapt to dynamic environmental risks. We introduced a memoryless, asymmetric self-preservation mechanism that allows agents to autonomously regulate their collision thresholds based on local interaction history.

Through systematic experiments (N=540 runs), we demonstrated that heterogeneous risk tolerances emerge spontaneously from identical agents interacting with their environment, converging to a physics-driven equilibrium. The adaptation asymmetry (α/β) serves as the control lever, where a "fast-panic, slow-relaxation" strategy is essential for system stability. However, stable differentiated equilibrium occurs only within a narrow parameter window around $\alpha/\beta \approx 5$. Outside this range, the system transitions to homogeneous risk-aversion ($\alpha/\beta \geq 10$) or collapses to risk-neutrality ($\alpha/\beta \leq 2.5$), revealing fragility in adaptive decentralized systems.

Theoretically, this work demonstrates how simple adaptive rules generate emergent coordination without centralized control. By mimicking biological heuristics, we achieve robust safety behaviors using only local binary stimuli. This suggests that complex collective coordination does not necessarily require complex individual cognition.

Future research should extend this work to 3D environments and real-world domains, while exploring limited inter-agent communication and heterogeneous initialization. Validation against empirical flocking data and investigation of whether heterogeneity improves collective performance also are important directions.

References

1. Ballerini, M., Cabibbo, N., Candelier, R., et al.: Interaction ruling animal collective behavior depends on topological rather than metric distance: Evidence from a field study of starling flocks. PNAS **105**(4), 1232–1237 (2008)
2. Brown, J.S., Laundré, J.W., Gurung, M.: The ecology of fear: optimal foraging, game theory, and trophic interactions. Journal of Mammalogy **80**(2), 385–399 (1999)
3. Couzin, I.D., Krause, J., Franks, N.R., Levin, S.A.: Effective leadership and decision-making in animal groups on the move. Nature **433**(7025), 513–516 (2005)
4. Couzin, I.D., Krause, J., James, R., Ruxton, G.D., Franks, N.R.: Collective memory and spatial sorting in animal groups. Journal of Theoretical Biology **218**(1), 1–11 (2002)
5. Dill, L.M.: Distance-to-cover and the escape decisions of an african cichlid fish. Environmental Biology of Fishes **27**(2), 147–152 (1990)

6. Farkas, I.J., Wang, S.: Spatial flocking: Control by speed, distance, noise and delay. PLOS ONE **13**(5), e0191745 (2018)
7. Gescheider, G.A.: Psychophysics: The Fundamentals. Lawrence Erlbaum Associates, Mahwah, NJ, 3rd ed. edn. (1997)
8. Gigerenzer, G., Gaissmaier, W.: Heuristic decision making. Annual Review of Psychology **62**, 451–482 (2011)
9. Griffin, A.S., Evans, C.S., Blumstein, D.T.: Learning specificity in acquired predator recognition. Animal Behaviour **62**(3), 577–589 (2001)
10. Harpaz, R., Tkačik, G., Schneidman, E.: Discrete modes of social information processing predict individual behavior of fish in a group. PNAS **114**(38), 10149–10154 (2017)
11. Hüttenrauch, M., Adrian, S., Neumann, G., Hoogendoorn, S.P.: Deep reinforcement learning for swarm systems. Journal of Machine Learning Research **20**(54), 1–31 (2019)
12. Kahneman, D., Tversky, A.: Prospect theory: An analysis of decision under risk. Econometrica **47**(2), 263–291 (1979)
13. Lima, S.L., Dill, L.M.: Behavioral decisions made under the risk of predation: A review and prospectus. Canadian Journal of Zoology **68**(4), 619–640 (1990)
14. Ling, H., Mclvor, G.E., van der Vaart, K., Vaughan, R.T., Thornton, A., Ouellette, N.T.: Costs and benefits of social relationships in the collective motion of bird flocks. Nature Ecology & Evolution **3**(6), 943–948 (2019)
15. Moussaïd, M., Helbing, D., Theraulaz, G.: How simple rules determine pedestrian behavior and crowd disasters. PNAS **108**(17), 6884–6888 (2011)
16. Papadopoulou, M., Hildenbrandt, H., Hemelrijk, C.K.: Diffusion during collective turns in bird flocks under predation. Frontiers in Ecology and Evolution **11**, 1198248 (2023)
17. Reynolds, C.W.: Flocks, herds and schools: A distributed behavioral model. In: Proceedings of the 14th Annual Conference on Computer Graphics and Interactive Techniques. pp. 25–34 (1987)
18. Schelling, T.C.: Micromotives and Macrobehavior. W. W. Norton & Company, New York, revised edition edn. (2006)
19. Schwarting, W., Alonso-Mora, J., Rus, D.: Planning and decision-making for autonomous vehicles. Annual Review of Control, Robotics, and Autonomous Systems **1**, 187–210 (2018)
20. Seitz, M.J., Bode, N.W., Köster, G.: How cognitive heuristics can explain social interactions in spatial movement. Journal of the Royal Society Interface **13**(121), 20160439 (2016)
21. Sridhar, V.H., Li, L., Gorbonos, D., Nagy, M., Schell, B.R., Sorochkin, T., Couzin, I.D.: The geometry of decision-making in individuals and collectives. PNAS **118**(50), e2102157118 (2021)
22. Sumpter, D.J.T.: The principles of collective animal behaviour. Philosophical Transactions of the Royal Society B: Biological Sciences **361**(1465), 5–22 (2006)
23. Vicsek, T., Czirók, A., Ben-Jacob, E., Cohen, I., Shochet, O.: Novel type of phase transition in a system of self-driven particles. Physical Review Letters **75**(6), 1226 (1995)
24. Wilensky, U.: Netlogo flocking model. Center for Connected Learning and Computer-Based Modeling, Northwestern University (1998), http://ccl.northwestern.edu/netlogo/models/Flocking
25. Wilensky, U.: Netlogo. Center for Connected Learning and Computer-Based Modeling, Northwestern University (1999), http://ccl.northwestern.edu/netlogo/